

Time-dependent structure in ultraviolet absorption lines of the rapid rotators HD 64760 (B0 Ib) and HD 93521 (O9.5 V)

Ian D. Howarth,¹ R. H. D. Townsend,¹ M. J. Clayton,¹ A. W. Fullerton,² D. R. Gies,³ D. Massa,⁴ R. K. Prinja¹ and A. H. N. Reid¹

¹ Department of Physics & Astronomy, University College London, Gower Street, London WC1E 6BT

² Center for Astrophysical Sciences, Department of Physics & Astronomy, The Johns Hopkins University, 3400 N. Charles St., Baltimore, MD 21218, USA

³ Center for High Angular Resolution Astronomy, Georgia State University, Atlanta, GA 30303, USA

⁴ Hughes STX, 7701 Greenbelt Road, Greenbelt, MD 20770, USA

Accepted 1998 January 6. Received 1997 December 23; in original form 1997 July 31

ABSTRACT

Cross-correlation provides an effective line-averaging function for spectra containing many line features, a result which can be exploited in order to perform time-series and spatial-domain analyses of absorption-line variability in data of (relatively) poor quality. We apply this method to high-resolution *IUE* spectra. For the known non-radial pulsator HD 93521 (O9.5 V), time-series analysis of the cross-correlation function recovers two periods that are confirmed in independent optical data ($P_1 = 1.77$ h, $P_2 = 2.90$ h); there is no statistically significant excess power at these frequencies in lines formed in the stellar wind. By comparing phase information from the time-series analysis with results from pulsation models we estimate $\ell \approx 10 \pm 1$ and 6 ± 1 as the harmonic degrees for P_1 and P_2 , respectively, with $\ell + m \leq 2$ for each mode (where m is the azimuthal order of the mode).

We also present evidence for absorption-line variability in HD 64760 (HR 3090; B0.5 Ib), finding marginally significant signals with $P_1 = 8.9$ h (or, possibly, 14.2 h) and $P_2 = 29$ h. The longer period is present, with a strong signal, in wind-formed lines. We consider possible circumstellar and (quasi-)photospheric origins for P_2 , and conclude that this signal probably does not arise through rotational modulation (with the corollary that the stellar-wind signal also does not arise in corotating structures, contrary to previous suggestions). The phase behaviour of the signals is consistent with non-radial pulsation models characterized by $\ell = 5 \pm 1$ (P_1) and 2 ± 1 (P_2), with $\ell + m \leq 1$, supporting a previous suggestion by Baade that both low- and higher-order modes are present; the wind modulation at P_2 may then result from leakage of pulsation energy into the supersonic outflow. The lack of significant photometric variability is a serious difficulty for this model (any sinusoidal photometric variability at P_2 has semiamplitude < 2 mmag at $\lambda_{\text{eff}} = 1575$ Å, with 95 per cent confidence), but this may itself be a consequence of wave leakage.

Key words: stars: early-type – stars: oscillations – ultraviolet: stars.

1 INTRODUCTION

Optical time-series spectroscopy of early-type stars has shown absorption-line variability at the ~ 1 per cent level to be rather common (e.g., Fullerton, Gies & Bolton 1996). Several mechanisms have been proposed that may give rise to this variability, including stochastic structure at the base of stellar winds, rotational modulation resulting from surface ‘spots’ of some description, or non-radial pulsation (see e.g. Fullerton et al. 1996; Balona 1991; and Gies 1991, respectively, for summaries). Although the signature of these processes is subtle, their diagnostic utility is considerable; this is especially true of non-radial pulsation (NRP), which offers the potential of asteroseismological analysis.

Observations of ultraviolet (UV) P Cygni profiles, in particular, have shown that variability is also an apparently ubiquitous characteristic of radiatively driven stellar winds, commonly taking the form of bluewards-propagating ‘discrete absorption components’, or DACs (e.g., Prinja & Howarth 1986, 1988; Kaper et al. 1996). A plausible mechanism for amplifying small seed signals at the base of a wind into observably large-scale phenomena at higher velocities is the radiative instability, extensively studied by Owocki and his collaborators (e.g., Owocki 1994). However, it is unclear whether stellar-wind variability is a direct response to a driving signal from the photospheric regions, or is self-initiating; in many cases the variability time-scales in the two regions are not commensurate (e.g., Howarth et al. 1993), while in others wind

variability is observed in stars having no detectable photospheric changes at all (see Fullerton et al. 1996). Indeed, it may be that, in at least some cases, the scattered radiation field in the wind can suppress the growth of signals input at the base of the outflow, and the importance of this effect may vary from star to star (Lucy 1984; Owocki 1994). Thus the so-called ‘photospheric connection’ between variability in the subsonic photosphere¹ and in the supersonic outflow remains unclear (even if the response is linear), in spite of a number of observational searches.

One straightforward approach to this question which is potentially capable of yielding clear-cut answers is to look for evidence of a common temporal signature in the photospheric spectrum and wind-formed lines. Reid & Howarth (1996) found such evidence in optical observations of the O4 supergiant ζ Puppis, identifying an 8.5-h signal in both the photospheric absorption lines *and* in the wind-formed H α profile, the latter at velocities well beyond $v_e \sin i$. However, the dominant signal at higher velocities has a ~ 19 -h period (Howarth, Prinja & Massa 1995), suggesting the base signal, presumed to result from pulsation, is damped, while the DACs may be self-initiating. To complicate matters further, a still longer period signal has been identified in the wind of ζ Pup, and has been associated with rotational modulation (Moffat & Michaud 1981; Howarth et al. 1995).

In the present paper we conduct a search for common temporal signatures in the winds and photospheres of two early-type stars, HD 64760 (HR 3090; CPD–47°1644) and HD 93521 (BD+38°2179). The former has, like ζ Pup, been reported as showing possible low-order non-radial pulsations (Baade 1984) as well as a rotationally modulated wind (Prinja, Massa & Fullerton 1995; Fullerton et al. 1997). Corotating circumstellar material may also be associated with HD 93521 (Howarth & Reid 1993), but it is of greater interest in the present context as a well-established non-radial pulsator (Fullerton, Gies & Bolton 1991; Howarth & Reid 1993).

2 OBSERVATIONS

The observational requirements for variability studies normally include both high spectral resolution (to address structure with high spatial frequencies) and extended, densely sampled time series (to facilitate time-series analysis). Spectra from the *International Ultraviolet Explorer* (*IUE*) provide a standard resource for investigating stellar-wind variability, for which a relatively low signal-to-noise ratio is adequate. However, quantitative analysis of *photospheric* line-profile variability normally also requires high signal-to-noise (*S/N*) ratio (because of the low amplitude of absorption-line changes). The rather low *S/N* ratio of the *IUE* data (typically ~ 20) therefore renders them generally unsuitable for direct investigation of the more subtle variability normally associated with photospheric absorption lines.

Under some circumstances this difficulty can be overcome by noting that the ultraviolet region offers a much larger number of strong photospheric lines of metals than does the optical; indeed, the range covered by *IUE*’s short-wavelength camera (~ 1150 – 2000\AA) is almost completely blanketed by such lines in O-type stars. Thus for a line width of $v_e \sin i \approx 200$ – 300 km s^{-1} the effective number of lines is $>10^2$ – a gain in excess of an order of

¹ For stars with slow, dense winds, in particular, it may not be true that all absorption lines are formed solely in such regions, but we will refer to such features as ‘photospheric’ as a convenience to distinguish them from P Cygni profiles and other obviously wind-formed lines.

Table 1. Summary of *IUE* observations.

	HD 64760	HD 93521
SWP image numbers	53339– 53781	50291– 50395
No. of observations	148	103
Start JD (–2 449 000)	730.8	432.6
Length of run (d)	15.77	2.94
Median time sampling (h)	2.15	0.60
Wavelength sampling (\AA)	0.1	0.1

magnitude over the optical. If these lines are equivalent from the point of view of line-profile variability, and if the information they contain can be combined, then in principle *S/N* ratios of several hundred can be achieved.

A straightforward and well-established technique for producing the required averaged profile is cross-correlation. The precise meaning of ‘averaged’ in this application is complicated by the weighting function introduced by the template spectrum with which any chosen target is correlated, but it is none the less evident that the cross-correlation process yields a function which is, in effect, an (inverted) mean line profile. This suggests the possibility of studying line-profile variability in the cross-correlation function (ccf), using standard techniques for time-series and spatial-domain analyses – a view encouraged by preliminary studies (Gies, unpublished work; Penny 1996; Howarth et al. 1997).

The choice of target is constrained by the availability of an appropriate template against which the target spectra may be cross-correlated; although one could, in principle, use model-atmosphere calculations to provide template spectra, our experiments in this direction suggest that real data give more satisfactory results at present. Since cross-correlation is, in effect, a convolution, then to preserve the spatial high-frequency content of the ccf requires that the linewidth in the template be as small as possible. However, there is a conspicuous deficit of narrow-lined stars at early spectral types (Conti & Ebbets 1977; Howarth et al. 1997), and only a few objects have the desirable property of intrinsic line widths less than *IUE*’s instrumental line-spread function, which is approximately Gaussian with $R \approx 10^4$. We have adopted τ Sco as the source of the template spectrum; this star is well known to have exceptionally narrow lines for its spectral type (Slettebak et al. 1975; Schönberner et al. 1988), and with a classification of B0.2 IV (Walborn 1971) gives a strong cross-correlation signal against target spectra from $\sim O7$ to $\sim B1$ (Howarth et al. 1997).

Our two targets were selected as being of astrophysical interest, and as both having spectral types close to the τ Sco template, large $v_e \sin i$ (to facilitate the examination of line-profile structure), and good time-series spectra available. The principal data sets, which were extracted by using *IUEDR* (Giddings et al. 1996), essentially in the manner described by Howarth & Prinja (1989), are summarized in Table 1.

3 STELLAR WIND VARIABILITY

3.1 Noise model

We have examined the spectra for signatures of periodic variability in the stellar winds and in the photospheres. In order to isolate those regions of spectra showing strong stellar wind variability, we first calculated noise models for each data set, following the methods described by Howarth & Smith (1995). An empirical estimate of the noise level as a function of wavelength and detected signal is

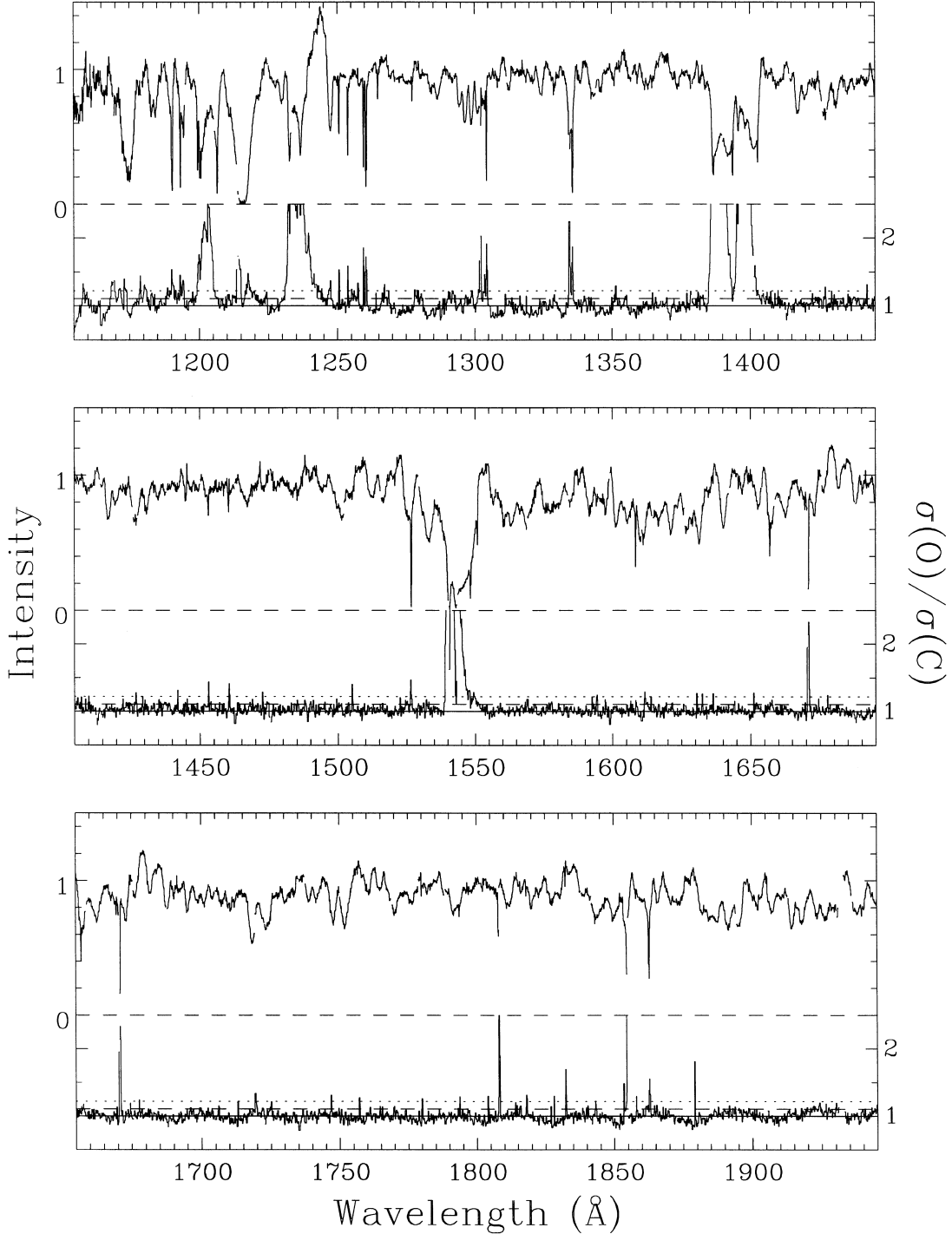


Figure 1. The mean spectrum for HD 64760 (upper panels) together with the ratio of observed to modelled standard deviations. The spectra have been rectified approximately, sampled at 0.1-Å steps, and lightly smoothed with a 3-point median filter. According to the χ^2 test, the null hypothesis of constancy can be rejected with, formally, 95 per cent confidence for points lying above the dashed line in the σ -ratio spectrum if there is an a priori expectation of variability, and with 95 per cent confidence for points above the dotted line if there is no such expectation. Very sharp features are generally because of undersampling of interstellar features or cosmic-ray events.

constructed from the data themselves, by assuming that there is no astrophysical contribution to the dispersion of the normalized data about their mean. This assumption is justified to the extent that the photospheric variability discussed in Section 4 is well below the noise level of individual data points, while regions subject to larger-amplitude variability are automatically excluded

from the noise model by an iterative sigma clip. A point-by-point comparison of the observed and modelled dispersions then provides a formal test of the confidence with which the null hypothesis of constancy can be rejected, using the χ^2 statistic, as in the ‘temporal variance spectrum’ described by Fullerton et al. (1996).

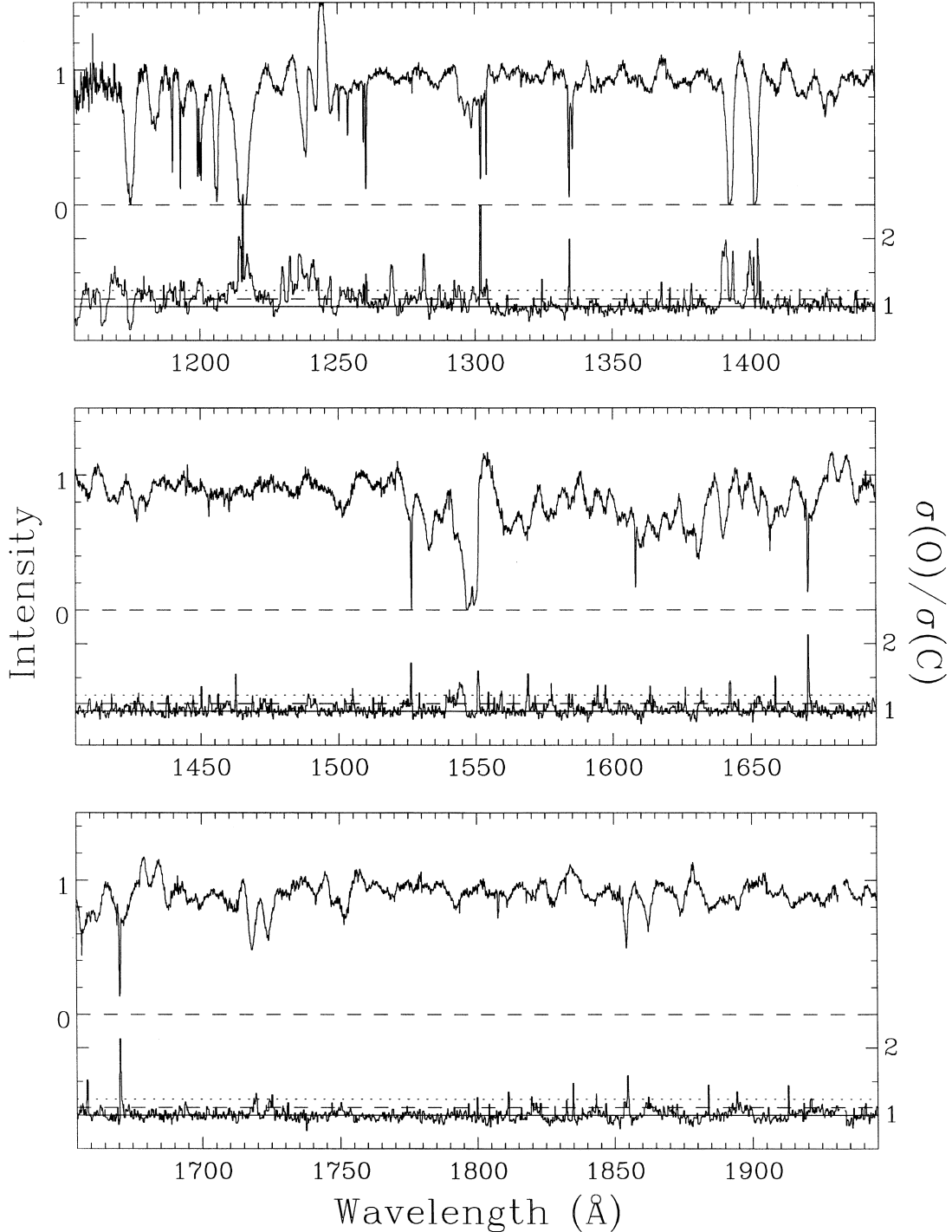


Figure 2. The mean and σ -ratio spectra for HD 93521; see Fig. 1 for details.

The results of the modelling are summarized in Figs 1 and 2. Examining the strong P Cygni profiles for which we have a priori grounds for supposing that variability may be present, we find that the χ^2 test allows us to reject the null hypothesis of constancy with >99 per cent confidence for the C IV $\lambda 1550\text{\AA}$, N V $\lambda 1240\text{\AA}$, and Si IV $\lambda 1400\text{\AA}$ doublets in both stars, and additionally for Si III $\lambda 1206.510\text{\AA}$ in HD 64760. Weak variability is known to occur in the C II $\lambda 1335\text{\AA}$ and Al III $\lambda 1960\text{\AA}$ resonance lines in HD 64760 (Massa, Prinja & Fullerton 1995), but χ^2 lacks the

efficiency (in the statistical sense) to identify it with confidence in the data used here.

P Cygni variability in HD 64760 extends from close to zero velocity out to (-1860 ± 50) km s $^{-1}$ in all four of its most strongly variable UV wind lines. HD 93521 shows slightly more diverse behaviour, resulting from the complex morphology of its equatorially compressed outflow (cf. Howarth & Reid 1993; Massa 1995; Bjorkman et al. 1994). C IV and Si IV are saturated out to about -300 km s $^{-1}$ (after correction for a

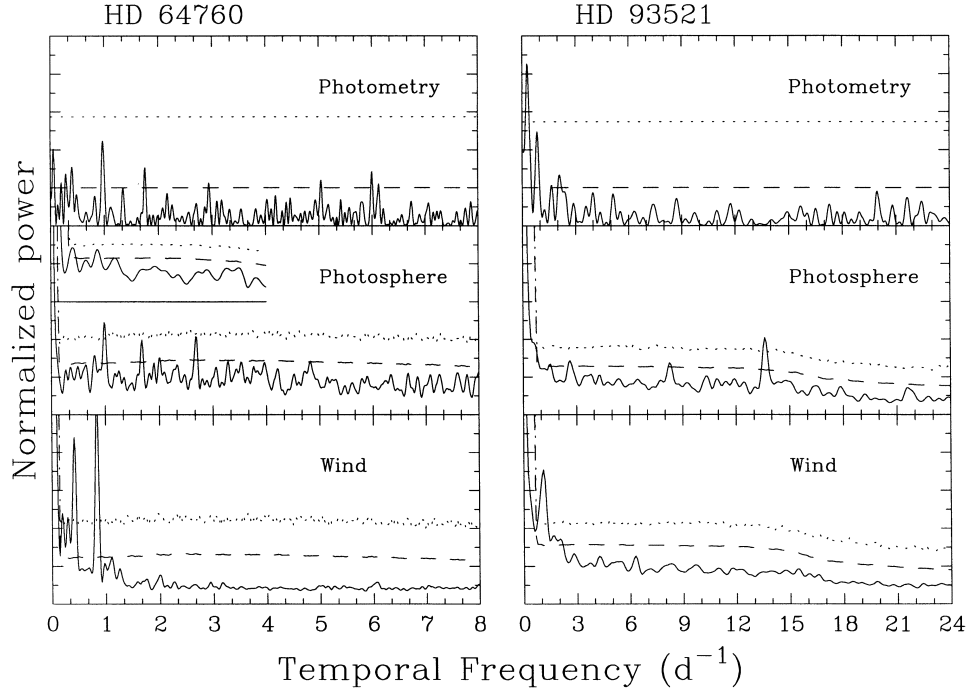


Figure 3. Time-series analysis of HDs 64760 and 93521. The upper panel shows the Lomb–Scargle periodogram of the integrated signal in the *IUE* data (with effective wavelengths of 1575Å for HD 64760 and 1593Å for HD 93521). The remaining panels show CLEAN periodograms for the cross-correlation functions (‘photosphere’) and stellar-wind lines, collapsed in the velocity/wavelength direction. The dashed lines indicate the levels above which a real signal may be claimed with 95 per cent confidence for a preselected frequency, and the dotted lines the 95 per cent confidence levels for *any* frequency. The offset photospheric power spectrum for HD 64760 shows results for an independent, shorter data set from 1993 (see Section 4.2.1).

stellar velocity of -30 km s^{-1}), which is close to the maximum outflow velocity in the equatorial plane, while both C IV and N V (though not Si IV) show formally significant variability out to about -1700 km s^{-1} , beyond the region of obvious P Cygni absorption.

3.2 Time-series analysis

We isolated those regions of the spectra showing formally significant variability according to the χ^2 test, and performed a time-series analysis of them using the implementation by Roberts, Lehar & Dreher (1987) of the CLEAN algorithm of Högbom (1974). The analysis proceeded in the manner described by Baade (1988a) and Gies & Kullavanijaya (1988), giving 2D periodograms of power as a function of wavelength and temporal frequency; we collapsed these in wavelength to obtain the power spectrum of any line-profile variability present. The results are shown in Fig. 3 (based on defaults of 50 CLEAN iterations with a gain of 0.8; we verified that the results are not sensitive to the choice of these parameters).

It is difficult to assess the statistical significance of peaks in the CLEANed, collapsed periodogram on an analytical basis. In order to estimate confidence levels we therefore used a simple Monte Carlo approach in which the times of the observations were held fixed, but the spectra associated with those times were randomly shuffled. The shuffled data sets were then processed as in the original analysis. This procedure was repeated 20 000 times, and probability levels estimated from the resulting cumulative distributions of power, frequency by frequency. These yield the probability p that a peak of given power (or greater) will occur by chance at a given frequency.

Because in general we have no a priori expectation of a significant signal at any particular frequency, we have to allow

for the fact that a large number of frequencies are scanned; thus the probability that a peak of given power (or greater) will occur by chance at *any* frequency is

$$p_N = 1 - (1 - p)^{N_i}, \quad (1)$$

where N_i is the number of independent frequencies examined. Horne & Baliunas (1986) suggest that $N_i \approx N$, the number of observations, for data uniformly sampled in time; we have explicitly verified this result for our data sets – which have almost uniform sampling – by repeating their analysis. Contours of constant probability are included in Fig. 3.

The widths of the peaks in the periodograms provide good estimates of the uncertainties on the frequency determinations when the excess power in the peaks is comparable to the noise levels (Schwarzenberg-Czerny 1991), as is generally the case for the present data. The half-power width is determined by the length of the observing run, D ; in the frequency domain, the full width at half-maximum (FWHM) is $\sim 1/D$, and we use this to provide error estimates.

Only one signal which is certainly of astrophysical origin² is present in the stellar wind data with >95 per cent confidence: a 1.2-d period (and a 2.4-d counterpart) for HD 64760. This period has already been reported in these data (Prinja et al. 1995), and is extensively discussed by Fullerton et al. (1997), who attribute it to spiral structures in the stellar wind and determine $P = 1.202 \pm 0.004 \text{ d}$. We will not, therefore, consider it further, other than in the context of the photospheric variability reported in the following sections.

² $\sim 1 \text{ d}^{-1}$ signals are found for HD 93521 (wind) and HD 64760 (photosphere and continuum). Similar signals are found in some other data sets, and are probably a consequence of diurnal (i.e., orbital) changes in the radiation-induced background level in *IUE* spectra.

4 PHOTOSPHERIC VARIABILITY

4.1 Cross-correlation methodology

Data processing, performed with `DIPSO` (Howarth et al. 1996), followed a simple standard ‘recipe’. For each target star we carried out the following steps.

(i) Interstellar lines and P Cygni lines were edited out of each spectrum, by multiplying the input data with a standard ‘window’ spectrum tailored to the star in question. (The ‘windows’ were designed to exclude all wavelengths within stellar-wind profiles – including potentially wind-contaminated features such as the Si III $\lambda 1300\text{\AA}$ complex – regardless of whether or not they showed statistically significant variability.)

(ii) The remaining data were divided by a standard (pseudo-) continuum function, scaled to the same mean value as the spectrum; final normalization was then carried out by fitting a low-order polynomial to the resulting rectified intensity spectrum, and subtracting the fit from the data. The spectra were ‘trimmed’ to remove regions at the shortest and longest wavelengths (which suffer from low S/N ratio and from interorder gaps, respectively).

(iii) Gaps in the data set resulting from editing were padded with zeroes, and the data at the edges of the gaps ramped to zero (over a 1- \AA interval), to damp edge effects.

The normalized spectra were then cross-correlated against a similarly processed τ Sco template. The resulting cross-correlation functions include a broad ‘pedestal’, but this is of no consequence for the analysis described in the following sections since it reproduces very well from spectrum to spectrum and, more importantly, is not a function of time.

To maximize the S/N ratio in the ccf, the cross-correlation functions were computed using large stretches of spectrum (1260–1900 \AA); thus scale errors and ‘drift’ in the wavelength calibration could moderate the sensitivity of the method. However, empirically we find that our extractions lead to interstellar-line wavelengths that are both reproducible and absolutely correct (with respect to laboratory wavelengths) at the sub-pixel level. Since the time-dependent features we find in the data have characteristic spectral scales which are upwards of an order of magnitude greater than this, the accuracy and precision of the wavelength calibration are not a cause for concern.

Analogous smearing of the ccf could arise if not all the lines we have isolated as ‘photospheric’ features are indeed formed at the same velocity; this is a particular danger in spectra of supergiants such as HD 64760 (cf. Massa & Prinja 1998). At present, we have no practical way of addressing this problem beyond a cautious approach to editing out features particularly prone to velocity shifts, but we note that the most likely effect of any residual astrophysical dispersion in line velocities is simply to reduce the S/N ratio in the ccf.

4.2 HD 64760

4.2.1 Time-series analysis

The ensemble of ccfs can be analysed using standard techniques for time-series analysis of spectroscopic data; we again used `CLEAN`. Although other techniques may easily be applied, Fourier-based methods (such as `CLEAN`) are attractive because they straightforwardly yield the phase of any near-coherent signal present; this information can be used to estimate mode parameters if the variability is interpreted in the context of non-radial pulsation (e.g., Gies & Kullivanijaya 1988; Telting & Schrijvers 1997).

The `CLEANED` ccf periodogram for HD 64760, collapsed over the range $\pm v_e \sin i$, is included in Fig. 3. (We do not present the uncollapsed 2D periodogram because it does not show any periodic signals that are obvious by simple visual inspection.) The length of the observing run results in rather good frequency resolution, although the sampling rate sets the pseudo-Nyquist frequency at only $\sim 8 \text{ d}^{-1}$. The only signal which can be identified with ~ 95 per cent confidence from the outset is at a frequency indistinguishable from 1 d^{-1} , and is unlikely to be of astrophysical origin.

The two next-strongest signals are at 1.68 and 2.68 d^{-1} ; these frequencies differ by $1.01 \pm 0.09 \text{ d}^{-1}$, and if either of them represents a true period then the other is evidently an alias. It is somewhat surprising, and disappointing, that aliasing should prove to be a problem, even with the use of the `CLEAN` algorithm, in such a well-sampled data set. Extensive testing with different values for the `CLEAN` gain and number of iterations, and with other period discriminants, does not resolve this ambiguity, but marginally favours the higher frequency insofar as it is generally associated with slightly greater power. Assuming that we have identified an astrophysical signal³, we therefore tentatively adopt $P_1 = 8.94 \pm 0.21 \text{ h}$ ($\nu = 2.68 \pm 0.06 \text{ d}^{-1}$), but cannot rule out $P_1 = 14.2 \text{ h}$. There is no evidence for any harmonic content at either period.

The next-highest peak in the power spectrum (and the only other peak above the dashed line in Fig. 3) is at $P_2 = 1.24 \pm 0.10 \text{ d}$ ($\nu_2 = 0.81 \pm 0.06 \text{ d}^{-1}$); that is, within the errors, at the same 1.2-d period present in the stellar wind periodogram. To investigate this signal further, we analysed 52 spectra obtained over a five-day interval in 1993 March (cf. Massa et al. 1995; Fullerton et al. 1997). The resulting power spectrum is included in Fig. 3, and shows a marginal 1.2-d signal, together with a slightly more convincing peak at 2.4 d (not present in the 1995 data). This behaviour parallels that in the high-velocity wind, which also shows more power at 2.4 d than at 1.2 d in the 1993 data (Fullerton et al. 1997). The 1993 data offer no support for a signal at P_1 .

From a purely statistical viewpoint, while the 1.2-d signal in the 1995 data set is only marginally significant in its own right, given the prior knowledge of the frequency (from the stellar wind analyses) the photospheric signal is significant at >99 per cent confidence. We therefore conclude that we have obtained a marginal detection of a possible short-period signal (P_1), and a secure detection of an absorption-line signal at the period observed in the stellar wind lines, P_2 . This, together with the linkages of behaviour in the 1993 and 1995 data sets, raises the concern that P_2 is the stellar-wind period, and results from contamination of absorption-line spectrum by lines formed partly in the outflow; we discuss this further in Section 5. We also note that if we have misidentified the shorter period, so that in fact $P_1 \approx 14 \text{ h}$, then the formal errors allow $P_2 = 2P_1$, suggesting that P_1 may simply be the first harmonic of P_2 . We return to this point in Section 4.2.4.

4.2.2 Mode identifications

Power and phase for both P_1 and P_2 are shown as a function of velocity in Fig. 4 for the 1995 data set (there are no important differences in the corresponding diagrams for $P_1 = 14.2 \text{ h}$). Compared to the noise level, the excess power resulting from the periodic signals is evidently rather modest at any given velocity,

³ The peaks in the power spectrum are significant at only ~ 90 per cent confidence, although preliminary examination of time-series data sets for a number of other stars has not yielded any comparably strong peaks.

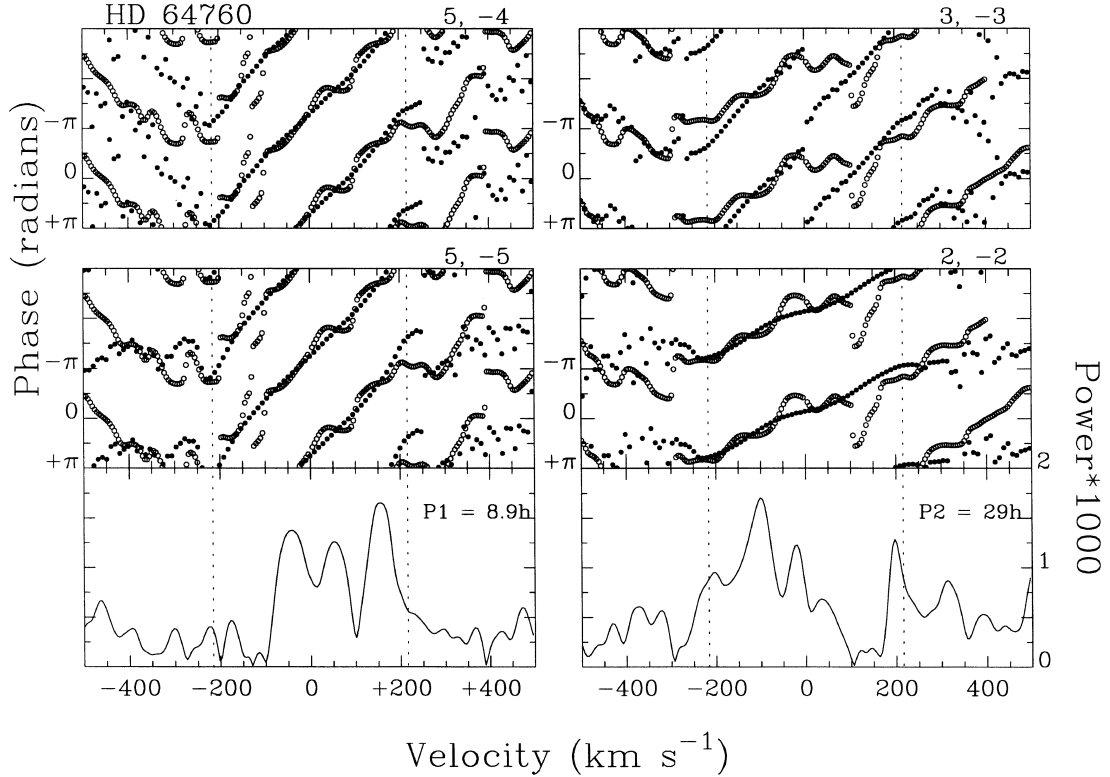


Figure 4. Phase (dots) and power (continuous lines) as a function of velocity for the two periods found in HD 64760. Phases are shown for the time of first observation, and are plotted with the ordinate ‘upside-down’ so that the pattern of variation matches that conventionally adopted for dynamic spectra. Observed phases in the cross-correlation function are shown as open circles, with phase variations for NRP models plotted as filled circles; the panels are labelled by the ℓ, m values of the corresponding models. Dashed vertical lines show $\pm v_e \sin i$, which is the range over which the model fits were performed. The best-fitting ($\ell, m = 5, -4$) and best-fitting sectoral models are shown for P_1 ; the lower panel for P_2 shows the best-fitting model, while the upper panel illustrates an alternative (and poorer) interpretation of the observed phase in the red wing relative to that bluewards of line centre. The coherence in phase diagrams outside the limits $\pm v_e \sin i$ is believed to result from extremely low-level systematic effects in rectification (for the models) and from partial correlation between unrelated features (in the observations).

Table 2. Physical parameters for target stars; ‘p’ and ‘e’ subscripts denote polar and equatorial values (where equatorial radii are calculated assuming a Roche model). Data are primarily adapted from Massa et al. (1995; HD 64760) and Howarth & Reid (1993; HD 93521); rotational velocities are from Howarth et al. (1997). Uncertainties on the parameters for HD 64760 are discussed in section 5.1; the (large) uncertainties for HD 93521 are discussed by Howarth & Reid (1993). For HD 64760 i , the inclination of the rotation axis to the line of sight, is inferred to be close to 90° because of the exceptionally large value of $v_e \sin(i)$.

	HD 64760	HD 93521
R_p/R_\odot	22	8.1
R_e/R_\odot	25.5	9.9
M/M_\odot	20	19
T_p (kK)	30	35
T_e (kK)	25.4	27.5
$\log g_p$ (cgs)	3.05	3.90
$v_e \sin i$ (km s $^{-1}$)	216	432
$P_{\text{rot}}/\sin i$ (d)	6.0	1.2
$\Omega/\Omega_{\text{crit}}$	0.64	0.73
i ($^\circ$)	85	85

and does not offer a useful diagnostic of the underlying processes; the 1993 data are still noisier, and will not be considered further. However, the systematic progress of phase across the line profile suggests the possibility of non-radial pulsation. (Rotational

modulation of surface features could give rise to a similar systematic progression, but such features would need to be located at regular intervals around the equator and, as we shall demonstrate, would need to possess prograde motion in the corotating frame.) To interpret the data in the context of NRP we have generated a grid of models, using Townsend’s BRUCE code (Townsend 1997). This code synthesizes line profiles in pulsating stars, taking full account of rotational effects on both the equilibrium stellar figure and on the pulsation-induced velocity, temperature, and geometric perturbations.

The stellar parameters required as inputs to the calculations are summarized in Table 2. (Note that, as a result of their rapid rotation, both stars experience significant equatorial extension and gravity darkening.) For the phase-diagram calculations, the maximum pulsation amplitudes were set at 10 km s^{-1} , which is an arbitrary but reasonable choice (less than, but of the order of, the sound speed). The intrinsic profiles are drawn from a precomputed grid of angle-dependent intensities from H/He non-LTE models (Smith & Howarth 1994), which renders impractical direct simulation of the cross-correlation results; we therefore calculated phase variations for the He I $\lambda 4713\text{\AA}$ line. Since the dominant lines in the 1000–2000 \AA region are from doubly ionized iron-group elements which, like the He I lines, continue to strengthen towards later spectral types, $\lambda 4713\text{\AA}$ is likely to be representative of the behaviour of most UV lines in terms of temperature sensitivity. The dependence of the modelled phase diagrams on temperature is, in any case, very small in the relevant region of parameter space.

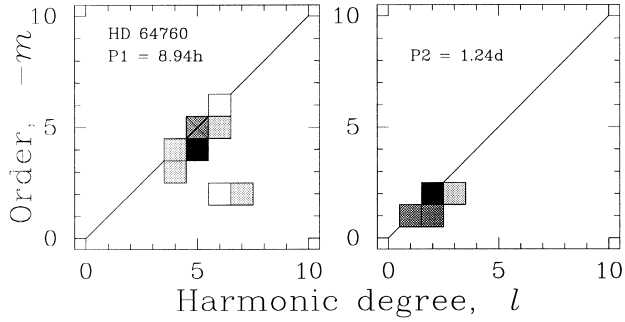


Figure 5. Summary of results of model fits to observed phase variations, as functions of harmonic degree ℓ and azimuthal order m , for HD 64760. The best-fitting solutions are shown in black; solutions which are judged poorer with less than 68, 95 and 99 per cent confidence are shown as dark grey, light grey, and white panels. The diagonal lines show the loci of sectoral modes; physically acceptable solutions must lie on or below this line, and the best-fitting sectoral-mode solution is marked with a cross where it does not coincide with the global best solution.

Our results confirm the finding by Telting & Schrijvers (1997) that the phase diagrams depend primarily on harmonic degree ℓ , and only weakly on azimuthal order m , for $|m| \approx \ell$. However, the physical treatments incorporated in the BRUCE models introduce more complex phase morphologies than the simple first-order perturbation-expansion models used by Telting & Schrijvers. This, together with the use of the complete phase pattern (rather than just the phase change across the profile), allows for reasonably sensitive discrimination of modes.

For a given mode, the phase offset between the observed and modelled phases can be estimated by minimizing the sum of the squares of the residuals, weighted by power in excess of the mean out-of-line power. (Other reasonable weighting schemes lead to negligibly different results.) The summed squared residuals also provide a discriminant which can be used in an F -test to assess the acceptability of non-optimal models. The results are summarized in Fig. 5. The best-fitting model for P_1 has $(\ell, -m) = (5, 4)$, but $(5, 5)$ gives a barely poorer fit to the phase diagrams (the claim that it is worse is supported with less than 1σ confidence), while the best-fitting model for P_2 has $\ell = -m = 2$. All solutions which are acceptable with 95 per cent confidence, bar one, are bracketed by $\ell = 5 \pm 1, 2 \pm 1$ for P_1 and P_2 , respectively, with $\ell + m \leq 1$. The results from this analysis of extensive but noisy data therefore support and quantify Baade’s (1984) examination of his sparse but precise optical spectroscopy, which, largely on the basis of line-profile structure, he interpreted as indicating a pair of low- and higher-order non-radial modes.

4.2.3 Photometry

Because we are unable to synthesize the cross-correlation function directly with our current models, the variability amplitude in the ccf is not a useful diagnostic of the physical amplitude of any pulsation present. The integrated flux provides an alternative handle on this quantity, and we have therefore carried out a time-series analysis of the *IUE* signal integrated over the range 1150–1950Å. Fig. 6 shows the light-curve, and the periodogram is included in Fig. 3. The dispersion in this *IUE* photometry is remarkably small – the standard deviation about the mean is only 0.6 per cent, or 6.6 mmag – but no significant peak is detected in the power spectrum.

By planting test signals in the data, we can determine upper limits to any periodic photometric variability present. We find that a

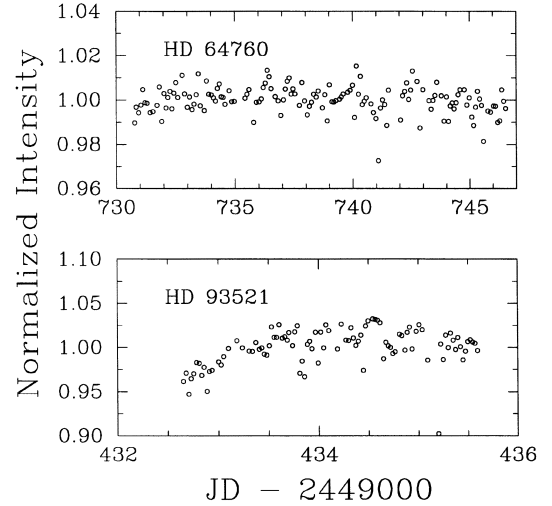


Figure 6. Ultraviolet photometry for HDs 64760 and 93521. Data points show the integrated *IUE* signals, normalized to the respective mean values; note that different scales are used in the two panels.

sinusoidal signal of semi-amplitude ≥ 0.2 per cent (2.2 mmag) with $P \approx 1.24$ d would be detected with 95 per cent confidence. The (single-mode) model calculations predict photometric variability of semi-amplitude $2.8[3.0] \times V_{\max}$ mmag for low-amplitude isothermal [adiabatic] pulsations, where V_{\max} is the maximum pulsation velocity in km s^{-1} . Taken at face value, therefore, the *IUE* photometry sets a very tight upper limit of $\sim 1 \text{ km s}^{-1}$ on the maximum velocity amplitude for an $\ell = -m = 2$ mode.

Adopting an $\ell, -m = (4, 4)$ model (for reasons discussed in Section 5) relaxes this substantially, predicting $0.1[0.6] \times V_{\max}$ mmag; the corresponding limits on the velocity amplitudes are $31 [5] \text{ km s}^{-1}$. However, the modelled phase diagram for this mode is inconsistent with the observed pattern at > 99 per cent confidence.

4.2.4 Caveats

It is important to note possible limitations on the modelling process. Both the Cowling approximation and the assumption of adiabaticity, implicit in the standard models, become unsatisfactory for the lowest-order modes, and $\ell \approx 2$ is marginal in this respect. However, the Cowling approximation is important primarily for calculating pressure perturbations at the surface, and becomes an increasingly good approximation as the surface is approached. The extent to which the adiabatic approximation is acceptable depends on the ratio of the cooling time-scale to the pulsation period in the corotating frame, and only for the 1.2-d period are any pulsations likely to be strongly non-adiabatic; in this case we have, where relevant, repeated our calculations assuming no temperature effects.

A more serious concern is that for low-order modes we may expect wave leakage through the adopted model boundary, and indeed the identification of the same period in the wind and photospheric signals provides evidence that leakage is occurring (Section 5). However, while leakage can significantly effect the calculation of horizontal velocity fields and of the temperature perturbations, and thereby introduce phase shifts in the models, the basic phase modulation that we use as a mode discriminant is unlikely to be otherwise seriously compromised by this effect.

Further potential uncertainty arises directly from the weakness of the observed signals. Because there is no significant power at P_2

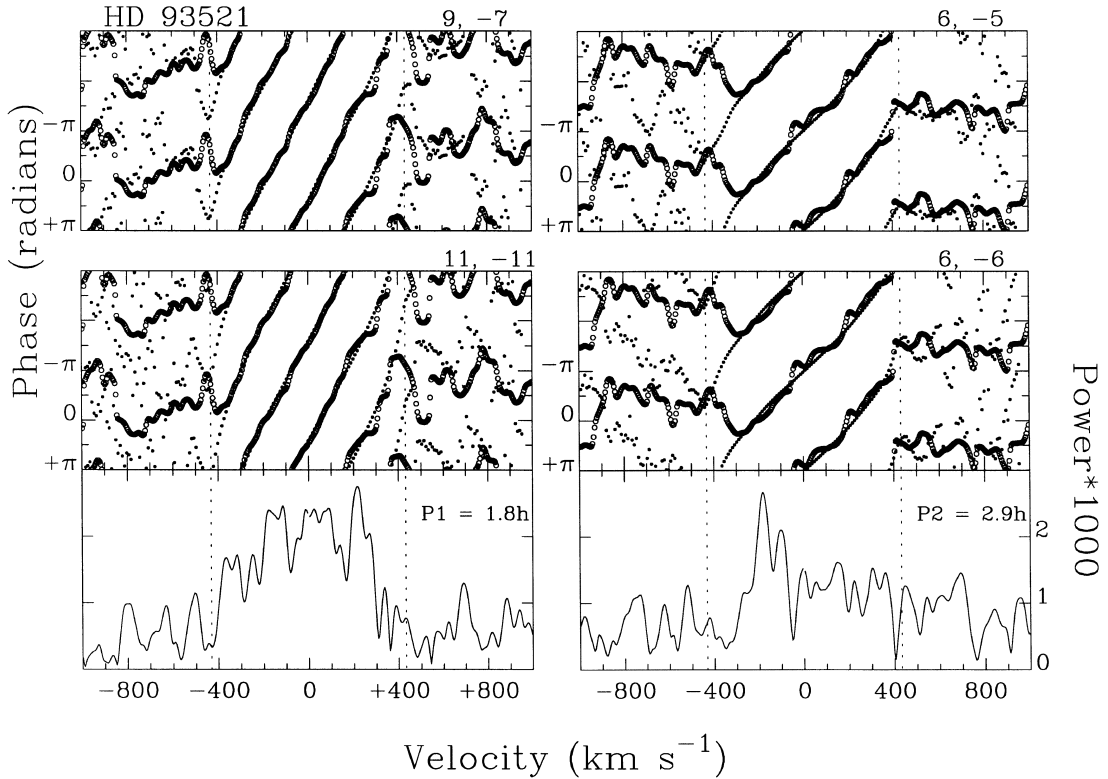


Figure 7. Phase (dots) and power (continuous lines) as a function of velocity for the two periods found in the cross-correlation function of HD 93521. Dashed vertical lines show the limits $\pm v_e \sin i$; other details are as Fig. 4.

between ~ 100 – 150 km s^{-1} redwards of line centre, the interpretation of the run of phase in that region is not secure (see Fig. 4). Consequently, there is a possible 2π ambiguity in the phasing of the red-wing signal relative to that bluewards of line centre. To investigate the importance of this ambiguity we repeated our analysis, but with observed phases redwards of 100 km s^{-1} increased by 2π . The best-fitting mode identification under this assumption is $\ell = -m = 3$, but the fit is poorer than our adopted model with greater than 95 per cent confidence; $(\ell, -m) = (4, 4)$, the next-best model, is a poorer fit than the $(3, 3)$ model with only ~ 90 per cent confidence, but is poorer than $(2, 2)$ with >99 per cent confidence. We conclude that, in the context of NRP, the correct interpretation of the data is most probably that which leads to the summary presented in Fig. 5.

A final point of concern is the relationship between the absorption-line periodicities; i.e., if P_1 is actually $\sim 14 \text{ h}$ (and not our preferred value of 8.9 h) then $P_2 \approx 2P_1$ (and $P_1 m_1 \approx P_2 m_2$). In that case the shorter-period signal, if real, may simply result from a non-sinusoidal component of the longer-period one. Other than marginally favouring $P_1 \approx 9 \text{ h}$, our data offer only a rather weak argument against this interpretation, in that P_1 shows relatively strong power in parts of the line profile where there is negligible power at P_2 (cf. Fig. 3). However, we also recall Baade’s (1984) study of his high-quality optical spectra; the *spatial* structure in those data supports the interpretation of *temporal* behaviour in the *IUE* spectra in terms of two quasi-independent signals.

4.3 HD 93521

4.3.1 Time-series analysis

The CLEANED ccf periodogram for HD 93521 is included in

Fig. 3. There is a statistically significant photospheric signal at 13.62 d^{-1} ($P_1 = 1.76 \pm 0.04 \text{ h}$), and weaker ones at 8.28 d^{-1} ($P_2 = 2.90 \pm 0.12 \text{ h}$) and 2.66 d^{-1} ($P_3 = 9.0 \pm 1.2 \text{ h}$). There is again no evidence for any harmonic content to any of these signals. The shorter period is indistinguishable from that reported by Fullerton et al. (1991) from data obtained in 1987, and by Howarth & Reid (1993) in echelle spectra taken with the 4.2-m William Herschel Telescope in 1992. P_2 has not been reported previously, but is confirmed in a new WHT data set obtained contemporaneously with the *IUE* observations (Reid et al., in preparation). Thus although only the short-period signal is formally significant (at the 95 per cent confidence level) when the *IUE* data are considered in isolation, both P_1 and P_2 are highly significant if the prior knowledge of the optical data is allowed. The case for an astrophysical signal underlying P_3 is less convincing (particularly since $\nu_1 \approx \nu_2 + 2\nu_3$); although Reid et al. find power at similar, although not identical, frequencies in optical data, the phase does not vary systematically with velocity in the UV cross-correlation results.

4.3.2 Mode identifications

Fig. 7 shows power and phase as a function of velocity for P_1 and P_2 . Modelling the phase as before we obtain $\ell \approx 10 \pm 1$ and 6 ± 1 as the harmonic degrees for P_1 and P_2 , respectively, with $\ell + m \leq 2$ (Fig. 8). This result is moderately sensitive to the adopted value for $v_e \sin i$, in part through second-order effects of rotation in the models, but primarily through simple scaling of the gradient of the modelled phase (or, equivalently, through the number of complete waves counted across the observed cross-correlation function). Adopting $v_e \sin i = 400 \text{ km s}^{-1}$ (Conti & Ebbets 1977) in place of 432 km s^{-1} reduces the estimated values of ℓ by ~ 1

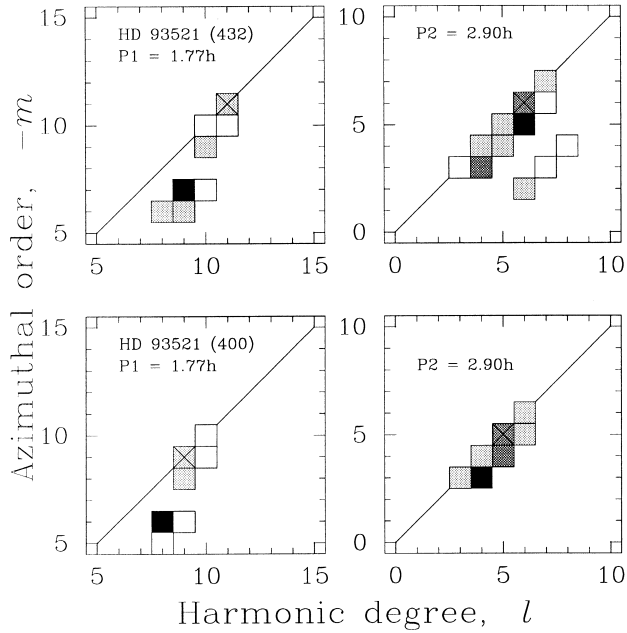


Figure 8. Summary of results of model fits to observed phase variations for HD 93521, as functions of harmonic degree ℓ and azimuthal order m ; details are as in Fig. 5. Families of solutions are shown for two values of $v_c \sin i$.

(Fig. 8). (The effect is less important for HD 64760 both because its rotation is slower and because the ℓ values are smaller.)

4.3.3 Photometry

Because the modes in HD 93521 are of relatively high order, integrated-flux variability does not usefully constrain the physical amplitudes. The data (Fig. 6, with a periodogram in Fig. 3) show a standard deviation about the mean of 2.1 per cent (22 mmag), and a signal of semi-amplitude 0.9 per cent (10 mmag) would be detected with 95 per cent confidence (for either period). Adiabatic models predict photometric semi-amplitudes at 1593\AA of $0.09V_{\max}$ and $0.16V_{\max}$ mmag for P_1 and P_2 respectively, so the data only rule out pulsation with amplitudes that are implausibly large (of order 10^2 km s^{-1}).

5 DISCUSSION

The *IUE* spectra we have studied in this paper have far poorer S/N ratio than data typically used to study absorption-line variability in OB stars. However, comparison of the present results for HD 93521 with observations made with the WHT confirms that the *IUE* spectra are capable of allowing a successful parameterization of that variability when the gain of the cross-correlation function is exploited; moreover, simultaneous stellar wind data are always at hand in these observations. We have shown that, when interpreted in the context of NRP, the phase diagrams for HD 93521 rule out models with many latitudinal nodes, but are consistent with sectoral ($\ell = |m|$) modes. (Of course, tesseral modes may also be present but undetected because of cancellation.) Both modes are prograde, with Ω/ω , the ratio of rotational to pulsational angular velocities, being 0.19 (P_1) and 0.26 (P_2).

While we have presented very tentative evidence for an ($\ell = |m| = 5$)-like signal for HD 64760, the most interesting result to emerge for this star is the identification of the 1.2-d stellar wind period in the absorption-line cross-correlation function.

The wind variability in this star has previously been linked with the photospheric rotation period on the grounds that $P_{\text{rot}} \approx 4P_2$ (Prinja et al. 1995; Owocki, Cranmer & Fullerton 1995; Fullerton et al. 1997), implying that there are four similar quadrants around the star (as in, for example, an $\ell = |m| = 4$ mode of pulsation). However, the phase diagram of the absorption-line variability, tacitly assumed to be associated with the photosphere, suggests that only *one* feature is visible in the cross-correlation function at a time (Fig. 4). This is consistent with corotation only if the material giving rise to the absorption-line signal in fact lies significantly *above* the photosphere; otherwise, if that signal is photospheric, then bilateral, not 4-fold, symmetry is implied. Of course, a third possibility is that the rather weak signal we have detected is spurious; however, its formal statistical significance is sufficiently high to encourage us to consider, in the following sections, the consequences of accepting at face value the phase diagram shown in Fig. 4. Nonetheless, the most secure conclusion of this paper is that additional, high-quality spectroscopy of HD 64760 is necessary in order to place the subsequent discussion on a firmer foundation (or to undermine it completely).

5.1 A circumstellar origin?

Material significantly above the photosphere could give rise to the P_2 signal we find in HD 64760 if it produced an absorption signature when seen in projection against the stellar disc. High-quality data could offer tests of this hypothesis (for example, the power should be almost constant across the line profile, and the phase change should be almost purely sinusoidal), but the *IUE* data are too noisy to provide useful diagnostics in this respect. However, they do offer some constraints; in particular, while the ccf signal may be blue-shifted by as much as $\sim 100\text{--}200 \text{ km s}^{-1}$, it is also consistent with symmetry about zero⁴ (Fig. 4). Since very large velocity shifts are apparently ruled out, we loosely categorize supraphotospheric models for the absorption-line variability as ‘circumstellar’, rather than ‘stellar wind’.

For $\sin i \approx 1$, circumstellar material that corotates and that has n -fold symmetry meets the requirement of one, and only one, feature in absorption at a time if it is organized into discrete ‘blobs’ at radial distance $R_*/\sin(\pi/n)$ from the centre of the star (that is, $1.15, 1.4$, or $1.5R_*$ for 3-, 4-, or 5-fold symmetry). In equator-on systems, the line-of-sight component of the tangential velocity of corotating material spans the range $\pm v_c \sin(i)$ while that material is projected against the photosphere (for any radial distance), which is consistent with the observed distribution of power in the ccf.

A difficulty with the corotation interpretation is in maintaining material in place with no significant radial velocity. A canonical wind-velocity law of the form $v \approx v_\infty(1 - R_*/r)^\beta$ gives $v \geq 0.3v_\infty (\approx 450 \text{ km s}^{-1})$ for $R \geq 1.4R_*$, $\beta \leq 1$; even 3-fold symmetry implies $v \geq 200 \text{ km s}^{-1}$. Such large velocity shifts are probably inconsistent with the observed characteristics of the 1.2-d absorption-line signal. They therefore render corotating material an unlikely explanation for that signal, although models where material is trapped at the appropriate points by ad hoc magnetic-field configurations cannot be ruled out on the basis of the present data.

⁴ A very crude quantitative justification for this statement is afforded by taking the running mean power averaged over $\pm v_c \sin i$; the averaged power at zero velocity is within 0.3σ of the maximum averaged power (which occurs at -160 km s^{-1}).

Table 3. Circumstellar models for n uniformly spaced ‘blobs’ around HD 64760.

n	P_{rec} (d)	R/R_{e}	$\pm v_{\text{proj}}$ (km s $^{-1}$)
2	1.67	1.00	387
3	1.38	1.15	312
4	1.40	1.41	230
5	1.48	1.70	174
6	1.57	2.00	137
7	1.67	2.30	111
8	1.76	2.61	92
9	1.85	2.92	77
10	1.94	3.24	66

However, there is no compelling reason to suppose that circumstellar material responsible for the 1.2-d period should strictly corotate, and previous interpretations of corotating stellar wind structures in HD 64760 are founded largely on plausibility arguments. The weakness of such arguments is exposed by noting that we must allow for at least a ~ 10 per cent uncertainty on the equatorial radius, R_{e} (HD 64760 is not known to be a cluster or association member, so that the radius is inferred solely from the spectral type), with a similar uncertainty on the equatorial rotation velocity, v_{e} , resulting from uncertainty in the inclination and, primarily, simple measurement error. Using the parameters from Table 2 then implies $P_{\text{rot}} = 6.0 \pm 0.8$ d. This is somewhat longer than previous estimates (Massa et al. 1995; Fullerton et al. 1997) both because we have used a better-documented source for $v_{\text{e}} \sin i$ (Howarth et al. 1997 in place of Hoffleit & Jaschek 1982; Slettebak et al. 1975 give 220 km s $^{-1}$) and because we have allowed for rotationally induced equatorial extension (Table 2). With these revisions we see that P_{rot} is almost exactly $5P_2$ (rather than $4P_2$); but also that even a minimum error budget will always allow an integer ratio of P_{rot} to P_2 within a 1σ range. Beyond consistency arguments, the ratio of these periods therefore has nothing to say regarding corotation or otherwise of features causing the cyclical variability observed in stellar-wind lines.

If we abandon the assumption of corotation, then Keplerian motion could offer an alternative method for maintaining circumstellar material in place without significant radial motion. Combining a circular orbit with the requirement that one ‘blob’ be in transit at a time leads to a unique solution for given n , as summarized in Table 3. No tabulated solution matches the strongest requirement, that the recurrence period P_{rec} ($= P_{\text{orb}}/n$) be 1.20 d, but this constraint is easily met by minor changes in the adopted stellar parameters, and most readily by changing the radius. For example, an equatorial radius of $23 R_{\odot}$ with $n = 4$ gives $P_{\text{rec}} = 1.20$ d, an orbital radius $R/R_{\text{e}} = 1.41$, and a radial velocity range while in transit of ± 242 km s $^{-1}$, consistent with observations.

5.2 A photospheric origin?

Although the Keplerian model can give rise to plausible parameters, it is completely ad hoc. Moreover, Keplerian ‘blobs’ orbiting at $\sim 1.4R_{\text{e}}$ would have somehow to resist both the radiation pressure driving the ambient wind, and the ram pressure of outflowing wind material with a relative velocity of $\approx 0.3v_{\infty}$.

A more natural explanation of the absorption-line signal is, therefore, that it originates in, or very close to, the photosphere. Moreover, the possibility of essentially bilateral symmetry at the time of the 1995 observations is to some extent supported by Fullerton et al.’s (1997) study of stellar wind variability, since they find that the

periodic component is largely accounted for by 1.2- and 2.4-d periods (see also Fig. 3); with bilateral symmetry, 2.4 d is the ‘superperiod’, mP , of the P_2 mode suggested here. The requirement that there be ~ 5 transits per rotation period, together with the blue-to-red migration of the phase pattern, then implies prograde motion of the features in the corotating frame ($\Omega/\omega = 0.36$).

As a caveat to this interpretation, we should note that Fullerton et al. (1997) recover the 2.4-d stellar wind period, but *not* the 1.2-d period, in the shorter data set obtained in 1993 March; our analysis of the ccf signal suggests similar behaviour in the absorption lines (Fig. 3). This indicates that the symmetry must be broken at some epochs. It could also be interpreted as suggesting that the ccf ‘photospheric’ signal is actually contaminated by the much stronger stellar wind variability; however, as noted previously, the velocity range of the observed excess power indicates that the signal probably originates close to the photosphere.

Although we have modelled the data in terms of non-radial pulsations, using Townsend’s (1997) code, this is simply a specific realization of the requirement that the underlying mechanism should lead to regular modulation of the line profile in such a way as to give one ‘feature’ visible at any given time. However, if we abandon a rotationally modulated model then we are naturally driven towards pulsation as an explanation. Unfortunately for the pulsation model, the limits which the photometry sets on the physical amplitude of a $(2, -2)$ mode represent a serious obstacle to this interpretation. Those limits translate into upper limits on the predicted profile variability of only ~ 1 part in 10^4 (rms) of the continuum level (for the He I $\lambda\lambda 4471, 4713$ lines), which would be well below our detection threshold. While increasing the corotating period decreases the photometric amplitude for a given pulsation amplitude (by enhancing transverse motions at the expense of radial movement, and hence decreasing the geometric effects which dominate the photometric changes), plausible changes in observational quantities (polar radius, $v_{\text{e}} \sin i$, P_2) have only minor consequences for the model predictions in this region of parameter space.

A similar difficulty is present for the O4 supergiant ζ Pup, which has also been reported as having a prograde ($\Omega/\omega = 0.19$) $\ell = |m| \approx 2$ mode (Baade 1988b; Reid & Howarth 1996), and which also lacks any corresponding photometric changes (Balona 1992). One possible solution is that the line-profile variability in these systems is a consequence of Rossby waves, the time-dependent analogue of the steady-state toroidal velocity fields found in non-rotating stars. Rossby waves have purely horizontal velocity fields, and so do not perturb the stellar radius; furthermore, owing to their solenoidal nature, they do not produce any temperature variations. Accordingly, they would be consistent with the lack of photometric variability.

There exists a significant stumbling block to this interpretation. The angular frequency of a Rossby wave with spherical-harmonic indices ℓ and m is given by

$$\omega \approx m\Omega \left[\frac{2}{\ell(\ell+1)} - 1 \right] \quad (2)$$

in an inertial frame (Papaloizou & Pringle 1978). By substituting appropriate values for ℓ , Ω , and ω , we solve for m to yield (ℓ, m) pairs which *could* describe the observations. We find that, for any reasonable ℓ values (and for reasonable ranges in Ω and ω), the values for m are such that $|m| > \ell$, which does not correspond to physically interesting solutions (formally, all spherical harmonics with $|m| > \ell$ are identically zero). Thus the Rossby-wave interpretation must be rejected.

There exists another way by which it may be possible to ‘salvage’ the NRP interpretation, which is to appeal to wave leakage through the photosphere. The BRUCE models follow Dziembowski’s (1971) formulation of the surface boundary condition, whereby it is assumed that the homology invariant $V \equiv -d \ln p / d \ln r$ is large at that boundary. In the case of systems with ‘abrupt’ surfaces, this assumption may be justified; however, its validity in the case of supergiants with dense winds is more dubious. Unno et al. (1989) have presented a more sophisticated formulation of the outer boundary conditions, which is better suited to treating systems with well-developed winds. The adoption of these boundary conditions leads to significant changes in the amplitudes of temperature perturbations and horizontal velocity fields with respect to Dziembowski’s formulation. In some cases, dependent on the physical parameters of the photosphere, Unno et al. describe a situation whereby the stellar surface is unable to reflect waves incident from the interior; these waves will leak through the photosphere and (presumably) out into wind regions, where they may act as a seed for variability.

The supergiants HD 64760 and ζ Pup appear to be strong candidates for such wave leakage, particularly in view of the empirical evidence for some form of pulsation/wind-variability connection in these two stars (and in the case of HD 64760, the evidence for related changes in the wind and ccf signals at different epochs). It may not be coincidental that $\ell = |m| = 2$ non-radial pulsations also appear to be a condition for rapidly-rotating B stars to show emission-line episodes (cf. e.g. Smith 1988), believed to be related to changes in their circumstellar environments. The wind structure of the supergiants, at least, may lead to a photosphere/wind boundary which is ill-defined, and thus poorly able to reflect outward-propagating waves. Accordingly, it is unlikely that Dziembowski’s boundary-condition formulation can accurately model the relative amplitudes of pulsation perturbations at the stellar surface for supergiants with dense winds, and so some discrepancy between model results and observations may be expected (even though it is probable that the mode identification itself is ‘safe’). Thus it would be premature to reject the NRP interpretation of low-order line-profile variability until further modelling of the wave-leakage phenomenon is undertaken. Cranmer (1996) has already presented some interesting results for base-perturbed winds, but there is a clear need for further work on a unified theory which treats the pulsation throughout star and wind on an equal footing.

ACKNOWLEDGMENTS

RHDT and AHNH were supported by PPARC, RKP by the Royal Society, and AWF by grant Pu 117/3-1 from the Deutsche Forschungsgemeinschaft. We thank Dietrich Baade for his considered and informed referee’s report.

REFERENCES

- Baade D., 1984, in Proc. 25th Liège International Astrophysical Colloq., Theoretical Problems in Stellar Stability and Oscillations. Université de Liège, Liège, p. 115
- Baade D., 1988a, in Cayrel de Strobel G., Spite M., eds, Proc. IAU Symp. 132, The Impact of Very High S/N Spectroscopy on Stellar Physics. Kluwer, Dordrecht p. 193
- Baade D., 1988b, in Conti P., Underhill A. B., eds, O Star and Wolf-Rayet Stars. NASA SP-497 p. 137
- Balona L. A., 1991, in Baade D., ed., Rapid Variability of OB-Stars: Nature and Diagnostic Value. ESO, Garching, p. 249
- Balona L. A., 1992, MNRAS, 254, 404
- Bjorkman J. E., Ignace R., Tripp T. M., Cassinelli J. P., 1994, ApJ, 435, 416
- Conti P. S., Ebbets D., 1977, ApJ, 213, 468
- Cranmer S., 1996, in Jeffery C. S., ed., CCP7 Newsl. no. 23, Spectroscopic Diagnostics of Small-Scale Structure in Stellar Atmospheres. Daresbury Laboratory p. 40
- Dziembowski W., 1971, Acta Astron., 21, 289
- Fullerton A. W., Gies D. R., Bolton C. T., 1991, BAAS, 23, 1379
- Fullerton A. W., Gies D. R., Bolton C. T., 1996, ApJS, 103, 475
- Fullerton A. W., Massa D., Prinja R. K., Owocki S., Cranmer S. R., 1997, A&A, 327, 699
- Giddings J., Rees P., Mills D., Clayton M., 1996, IUEDR (Starlink User Note 37). Rutherford Appleton Laboratory
- Gies D. R., 1991, in Baade D., ed., Rapid Variability of OB-Stars: Nature and Diagnostic Value. ESO, Garching, p. 229
- Gies D. R., Kullavanijaya A., 1988, ApJ, 326, 813
- Hoffleit D., Jaschek C., 1982, The Bright Star Catalogue. Yale University Press, New Haven
- Högbom J. A., 1974, ApJS, 15, 417
- Horne J. H., Baliunas S. L., 1986, ApJ, 302, 757
- Howarth I. D., Murray J., Mills D., Berry D. S., 1996, DIPSO (Starlink User Note 50). Rutherford Appleton Laboratory
- Howarth I. D. et al., 1993, ApJ, 417, 338
- Howarth I. D., Prinja R. K., 1989, ApJS, 69, 527
- Howarth I. D., Prinja R. K., Massa D., 1995, ApJ, 452, L65
- Howarth I. D., Reid A. H. N., 1993, A&A, 279, 148
- Howarth I. D., Siebert K. W., Hussain G. A. J., Prinja R. K., 1997, MNRAS, 284, 265
- Howarth I. D., Smith K. C., 1995, ApJ, 439, 431
- Kaper L., Henrichs H. F., Nichols J. S., Snoek L. C., Volten H., Zwarthoed G. A. A., 1996, A&AS, 116, 275
- Lucy L. B., 1984, ApJ, 284, 351
- Massa D., 1995, ApJ, 438, 376
- Massa D., Prinja R. K., Fullerton A. W., 1995, ApJ, 452, 842
- Massa D., Prinja R. K., 1998, in Howarth I. D., ed., Boulder-Munich II: Properties of Hot, Luminous Stars. Astron. Soc. Pac., San Francisco p. 208
- Moffat A. F. J., Michaud G., 1981, ApJ, 251, 133
- Owocki S. P., 1994, ApSS, 221, 3
- Owocki S. P., Cranmer S. R., Fullerton A. W., 1995, ApJ, 453, L370
- Papaloizou J., Pringle J. E., 1978, MNRAS, 182, 423
- Penny L. R., 1996, ApJ, 463, 737
- Prinja R. K., Howarth I. D., 1986, ApJS, 61, 357
- Prinja R. K., Howarth I. D., 1988, MNRAS, 233, 123
- Prinja R. K., Massa D., Fullerton A. W., 1995, ApJ, 452, L61
- Reid A. H. N., Howarth I. D., 1996, A&A, 311, 616
- Roberts D. H., Lehar J., Dreher J. W., 1987, AJ, 93, 698
- Schönberner D., Herrero A., Becker S., Eber F., Butler K., Kudritzki R. P., Simon K. P., 1988, A&A, 197, 209
- Schwarzenberg-Czerny A., 1991, MNRAS, 253, 198
- Slettebak A., Collins G. W., Boyce P. B., White N. M., Parkinson T. D., 1975, ApJS, 29, 137
- Smith K. C., Howarth I. D., 1994, A&A 290, 868
- Smith M. A., 1988, in Stalio R., Willson L. A., eds, Pulsation & Mass Loss in Stars. Kluwer, Dordrecht p. 251
- Teltung J. H., Schrijvers C., 1997, A&A 317, 723
- Townsend R. H. D., 1997, MNRAS, 284, 839
- Unno W., Osaki Y., Ando H., Saio H., Shibahashi H., 1989, Nonradial Oscillations of Stars. University of Tokyo Press, Tokyo
- Walborn N. R., 1971, ApJS, 23, 257

This paper has been typeset from a $T_{\text{E}}X/L^{\text{A}}T_{\text{E}}X$ file prepared by the author.